Coverage Analysis for Backscatter Communication Empowered Cellular Internet-of-Things

Syed Ali Raza Zaidi, Maryam Hafeez, Des McLernon and Moe Z. Win

Invited Paper

***Abstract*—In this article, we develop a comprehensive framework to characterize the coverage probability of backscatter communication empowered cellular Internet-of-Things (IoT) sensor networks (SNs). The developed framework considers hierarchical cellular type deployment topology which is practically useful for various IoT applications. In contrast to existing studies, the framework is geared towards system level performance analysis. Our analysis explicitly considers the dyadic fading experienced by the links and spatial randomness of the network nodes. To ensure tractability of analysis, we develop novel closed-form bounds for quantifying the coverage probability of SNs. The developed framework is corroborated using Monte Carlo simulations. Lastly, we also demonstrate the impact of various underlying parameters and highlight the utility of the derived expressions for network dimensioning.**

***Index Terms*—backscatter communication, dyadic fading, stochastic geometry, Poisson process, coverage probability.**

I. Introduction

A. Motivation

THE foundation of Internet-of-Things (IoT) is based on Weiser's vision of profound software/hardware technologies that weave themselves into the fabric of everyday life such that they become indistinguishable. The functionality and modalities of these technologies is distributed across a variety of interconnected objects. This inter-connectivity of objects is pivotal as the collective intelligence of the IoT network emerges from simple object level interactions. Ericsson's recent forecast predicts that there will 1.5 billion IoT devices with cellular connections by 2022. While cellular topology allows efficient deployment of IoT sensor nodes (SNs), connectivity to existing cellular base stations (BSs) is power hungry even with the state-of-the-art Narrowband IoT (NB-IoT) radio technology. With the massive volume of devices, it is essential to explore energy efficient (EE) SN design as recharging the deployed SNs individually on regular basis might be impractical.

One way to realize the EE design is to actually harvest energy from ambient RF signals and then utilize harvested energy to drive the transceiver on sensor boards [1]. This design can be further refined by employing RF backscatter based communication which is based on the RF reflection principle. Backscatter radio achieves data transmission from SNs by modulating information onto the illuminating RF carrier signal. The RF carrier modulation is achieved by connecting an antenna to different loads which fundamentally translates into different antenna-load reflection coefficients (see Section 2). Backscatter radios can realize power consumption of the order of μWatts for IoT SNs, mainly because the SN design does not require expensive analog components such as RF oscillators, mixers, crystals and decoupling capacitors etc. Interested readers are referred to a recent tutorial on Backscatter based IoT SN design in [2]. Optimal dimensioning of Backscatter based IoT SNs requires a statistical framework to model such network deployments and subsequently quantify the impact of various underlying parameters on the achievable performance. In contrast to traditional wireless networks, the SNs experience a dyadic channel which is formed by a combination of forward channel (from SN to access point (AP)/carrier emitter(CE)) and backward channel (from AP to SN). In [3], the authors have considered dyadic fading channel and characterized the performance of a single AP which is serving multiple SNs. The authors have also explored collision resolution techniques to improve the performance. The analysis presented in [3] even for a single AP does not admit a closed-form solution for the considered performance metric (decoding/coverage probability) and requires several folds of numerical integration. This obscures insights into how the considered performance metric is effected by different parameters such as node density, path-loss exponent, desired signal-to-interference-ratio (SIR) threshold, etc. The analysis cannot be extended to a more realistic scenario where multiple APs are deployed such that each AP only serves the nearby SNs. Such a topology is required to realize applications like smart farms where multiple APs are deployed, each serving several soil moisture SNs to provide a certain fidelity for the coverage. Similar topologies arise in other applications such as air-quality monitoring where sensors are spread across a wider geographical region. In [4], the authors considered multiple APs and SNs for Backscatter based IoT networks and developed a framework for performance analysis. However, the developed framework ignores the dyadic fading experienced by the SN transmissions. A related line of work explores backscattering via ambient RF signals. The interested reader is directed to [5] for a detailed survey of ambient backscatter communication.

B. Contribution & Organization

In this article, we develop a statistical framework for quantifying the performance of a backscatter based cellular IoT network in terms of the coverage probability (see Section 3). We develop novel closed-form bounds on the coverage probability of SNs which are tractable and do not require any numerical integration (Section 3). Our proposed framework explicitly accommodates the properties of dyadic fading channel whereby the forward and the backward channel can experience non-zero

S. A. R. Zaidi and D. C. McLernon are with the School of Electronic and Electrical Engineering, the Univesity of Leeds, UK. M. Hafeez is affiliated with the School of Engineering and Computer Sciences at the University of Huddersfield. M. Z. Win is with the Laboratory of Information and Decision Systems (LIDS), Massachusetts Institute of Technology (MIT), Cambridge, Massachusetts, USA. Emails:{s.a.zaidi@leeds.ac.uk, m.hafeez@hud.ac.uk, moewin@mit.edu}. This research is supported by the Research England QR Global Challenges Research Fund and in part by the National Science Foundation under Grant CCF-1525705.

978-9-0827-9703-9/19/$31.00 ©2019 IEEE

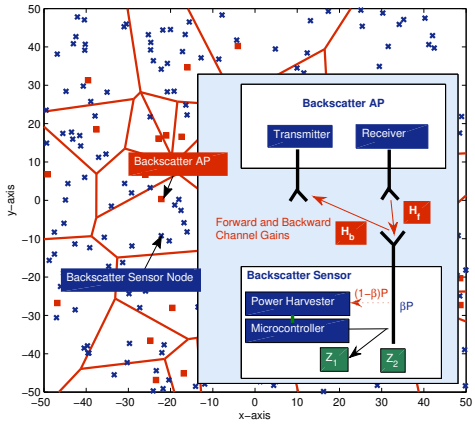

Fig. 1. Network Model and Architecture of Backscatter AP and SN.

correlation. We also incorporate the spatial randomness of SNs and APs in our analysis via stochastic geometric modeling (see Section 2). We corroborate the developed framework with the help of Monte Carlo simulations (see Section 4) and briefly explore how the analysis can be employed for dimensioning backscatter based IoT networks.

II. System Model

A. Spatial Model

We consider a cellular deployment of backscattered APs as shown in Fig. 1. The spatial distribution of both APs and SNs is captured by a two independent *homogeneous Poisson point processes* (HPPPs) $\Pi_{AP} \in \mathbb{R}^2$ with intensity λ_{AP} and $\Pi_{SN} \in \mathbb{R}^2$ with intensity λ_{SN} respectively [6]. The parameter $\lambda_{AP}(\lambda_{SN})$ is the average number of APs/SNs per unit area. It is assumed that each AP serves the SNs inside its Voronoi cell.

B. Channel Model

All links are assumed to experience large scale path-loss along with small-scale block fading. A backscatter channel is dyadic in nature, i.e., the reflected signal experiences a channel gain which is a product ($\mathcal{H} = \mathcal{H}_f\mathcal{H}_b$) of forward channel (AP-to-SN) gain ($\mathcal{H}_f = \|\boldsymbol{G}_f\|^2$) and backward channel (SN-to-AP) gain $\mathcal{H}_b = \|\boldsymbol{G}_b\|^2$, where, $\boldsymbol{G}_i \sim \mathcal{CN}(0,1), i = \{f, b\}$ with non-zero correlation $\rho = \mathbb{E}(\boldsymbol{G}_f\boldsymbol{G}_b)$. In other words, the two links as shown in Fig. 1 are correlated with a correlation factor $\rho \in [0,1]$. The overall channel gain between a transmitter and a receiver separated by a distance r is denoted as $\mathcal{H}l(r) = \mathcal{H}_f\mathcal{H}_b l(r)$ where $l(r) = Cr^{-\alpha}$ is the power-law path-loss function. The path-loss function depends on the distance r, a frequency dependent constant C and an environment/terrain dependent path-loss exponent α. The fading channel gains are assumed to be mutually independent and identically distributed (i.i.d.) across different links, i.e. $\mathbb{E}(\mathcal{H}_i, \mathcal{H}_j) = 0 \, \forall i \neq j$. Without any loss of generality, we will assume $C = 1$ for the rest of this discussion.

C. Backscatter Communication

We consider mono-static backscattering APs whereby both transmit and receive antennas are co-located. The AP transmits an unmodulated RF signal $s(t) = \sqrt{2P}\exp\left(-i\left(\omega_c t + \phi_c\right)\right)$ where $i = \sqrt{-1}$ $\omega_c = 2\pi f_c$ is the angular frequency corresponding to the carrier frequency, ϕ_c is carrier phase and $\mathbb{E}(s^2(t)) = P$ (watts) is the transmit power. It is assumed that the transmit power is fixed to the maximum permissible level under regulatory constraints at the desired transmission frequency f_c (Hz). The SN reflects back the received signal $y(t) = \sqrt{2Pl(r)}\boldsymbol{G}_f \exp\left(-i\left(\omega_c t + \phi_c\right)\right)$ using the same antenna which is used to receive $s(t)$. The sensor data payload is modulated onto the reflected signal by varying the reflection coefficient $\beta(t) = \beta_m b(t)$ through load modulation, where $b(t)$ is the binary function of time which only assumes ± 1 values. The parameter β_m is coupled with several hardware design related factors. The reflected signal received at the AP from an SN (say o) separated by distance r_o is given by, $y_{AP}(t) = \boldsymbol{G}_f^o\boldsymbol{G}_b^o l(r_0)\beta_m b_o(t)s(t) + \sum_{j\neq o\in\Pi_{SN}} \boldsymbol{G}_f^j\boldsymbol{G}_b^j l(r_j)\beta_m b_j(t)s(t) + n(t)$.Consequently, the received SINR for a fixed $b(t)$ corresponding to either binary symbol $\{0,1\}$ is given as,

$$\text{SINR} = \Gamma = \frac{\overbrace{Pl^2(r_o)\mathcal{H}_f^o\mathcal{H}_b^o\beta}^{\text{Desired SN signal power}}}{\underbrace{\sigma^2}_{\text{AWGN Noise Power}} + \underbrace{\sum_{j\neq o\in\Pi_{SN}} Pl^2(r_j)\mathcal{H}_f^j\mathcal{H}_b^j\beta}_{\text{Interference from other SNs}}}, \tag{1}$$

where $\beta = \|\beta_m\|^2 \in [0,1]$, is the reflection coefficient. Here we assume that each AP uses a different carrier frequency f_c and consequently there is no power aggregation at SNs from out-of-cell APs. However as SNs are not aware of the f_c, the out-of-cell SNs will contribute to co-channel interference.

III. Performance Analysis

A. Dyadic Rayleigh Fading Channel

Consider the small-scale fading experienced on the forward and backward propagation channel, which is modeled by two complex Gaussian random variables $\boldsymbol{G}_f \triangleq G_f^{(I)} + iG_f^{(Q)}$ and $\boldsymbol{G}_b \triangleq G_b^{(I)} + iG_b^{(Q)}$ where $i = \sqrt{-1}$. Moreover, from the assumption that $\mathbb{E}(\boldsymbol{G}_f) = \mathbb{E}(\boldsymbol{G}_b) = 0$, it follows that,

$$\mathbb{E}(G_f^{(I)}) = \mathbb{E}(G_f^{(Q)}) = \mathbb{E}(G_b^{(I)}) = \mathbb{E}(G_b^{(Q)}) = 0.$$

The co-variance matrix of is of the form of [7]

$$C_{\boldsymbol{G}_f\boldsymbol{G}_b} = \begin{bmatrix} \sigma_f^2 & 0 & \sigma_f\sigma_b\rho_c & \sigma_f\sigma_b\rho_s \\ 0 & \sigma_f^2 & -\sigma_f\sigma_b\rho_s & \sigma_f\sigma_b\rho_c \\ \sigma_f\sigma_b\rho_c & -\sigma_f\sigma_b\rho_s & \sigma_b^2 & 0 \\ \sigma_f\sigma_b\rho_s & \sigma_f\sigma_b\rho_c & 0 & \sigma_b^2 \end{bmatrix}, \tag{2}$$

where $|\rho_c| \leq 1$ and $|\rho_s| \leq 1$ are the correlation coefficients between the in-phase and quadrature components. Under these assumptions the reflected signal received on the AP experiences bi-variate Rayleigh fading, i.e., $\bar{G}_f = \sqrt{\left(G_f^{(I)}\right)^2 + \left(G_f^{(Q)}\right)^2}$ and $\bar{G}_b = \sqrt{\left(G_b^{(I)}\right)^2 + \left(G_b^{(Q)}\right)^2}$ have a joint bi-variate Rayleigh distribution given by [8]

$$f_{\bar{G}_f\bar{G}_b}(g_f, g_b) = \frac{g_f g_b}{\sigma_f^2\sigma_b^2\left(1-\rho^2\right)} \exp\left(-\frac{\left[\frac{g_f^2}{\sigma_f^2} + \frac{g_b^2}{\sigma_b^2}\right]}{2\left(1-\rho^2\right)}\right) \times \mathcal{I}_0\left(\frac{\rho g_f g_b}{\left(1-\rho^2\right)\sigma_f\sigma_b}\right), \quad g_f, g_b \geq 0, 1 \leq |\rho|, \tag{3}$$

where $\tilde{\rho} = 1-\rho^2$, $\rho^2 = \rho_c^2 + \rho_s^2$ and $\mathcal{I}_0(x) = \frac{1}{\pi}\int_0^{\pi}\exp(-x\cos(t))dt$,is the zeroth order modified Bessel function of first kind. Joint moments of $\bar{G}_f$ and $\bar{G}_b$ of the form $\mathbb{E}(\bar{G}_f^n \bar{G}_b^m), n+m = 1,2,..$ were first calculated by Middleton in [7] as

$$\begin{aligned} \mathbb{E}(\bar{G}_f) = \sigma_f\sqrt{\pi/2}, \quad \mathbb{E}(\bar{G}_b) = \sigma_b\sqrt{\pi/2}\ , \\ \mathbb{E}\left(\bar{G}_f^2\right) = 2\sigma_f^2, \quad \mathbb{E}\left(\bar{G}_b^2\right) = 2\sigma_b^2, \\ \mathbb{E}\left(\bar{G}_f\bar{G}_b\right) = \sigma_f\sigma_b\left[2\mathrm{E}(\rho) - (1-\rho^2)\mathrm{K}(\rho)\right], \end{aligned} \tag{4}$$

where $\mathrm{K}(x)$ and $\mathrm{E}(x)$ are complete Elliptic Integrals of first and second kind respectively. Employing the Eq. (4) the correlation of variable $\bar{G}_f$ and $\bar{G}_b$ is given

$$\bar{\rho} = \frac{\mathbb{E}(\bar{G}_f\bar{G}_b)}{\sigma_f\sigma_b} = 2\mathrm{E}(\rho) - (1-\rho^2)\mathrm{K}(\rho). \tag{5}$$

Clearly $\bar{\rho} \neq \rho$ and thus there have been several attempts (see [9]-[10]) to develop algorithms to simulate dependent Rayleigh random variables with a certain given cross-correlation $\bar{\rho}$. Generally generation exploits a coloring matrix which is obtained via Cholesky decomposition of correlation matrix of underlying Gaussian process. Interested readers are referred to [10] for details. It is important to highlight that some prior studies (which employ analysis in [11], where ρ has different definition) have confused $\bar{\rho}$ with the cross-correlation factor of underlying complex Gaussian random variable ρ resulting in an erroneous analysis of considered performance metric.

Remark 1: In general $\mathbb{E}(f(\boldsymbol{G}_f)f(\boldsymbol{G}_b)) \neq \mathbb{E}(\boldsymbol{G}_f\boldsymbol{G}_b)$; from this it follows that the correlation coefficient ($\bar{\rho}$) of the bi-variate Rayleigh fading channel amplitude has a non-linear relationship with the correlation coefficient (ρ) of the corresponding complex Gaussian channel gain as demonstrated in Eq. (4).

Characterization of the coverage probability of the backscatter powered sensor node requires the PDF and CDF for the dyadic fading channel, i.e., $\mathcal{H} = \mathcal{H}_f\mathcal{H}_b$ where $\mathcal{H}_f = \|\boldsymbol{G}_f\|^2$ and $\mathcal{H}_b = \|\boldsymbol{G}_b\|^2$. The joint distribution of $\mathcal{H}_f\mathcal{H}_b$ from the Eq. (3) using the standard change of variables as:

$$\begin{aligned} f_{\mathcal{H}_f,\mathcal{H}_b}(h_f,h_b;\rho) = \frac{1}{4\tilde{\rho}\sigma_f^2\sigma_b^2}\exp\left(-\frac{1}{2\tilde{\rho}}\left[\frac{h_f}{\sigma_f^2}+\frac{h_b}{\sigma_b^2}\right]\right) \\ \times\mathcal{I}_0\left(\frac{\rho\sqrt{h_fh_b}}{\tilde{\rho}\sigma_f\sigma_b}\right), \end{aligned} \tag{6}$$

The PDF of $\mathcal{H} = \mathcal{H}_f\mathcal{H}_b$ is obtained as,

$$f_{\mathcal{H}}(h) = \int_{-\infty}^{\infty}\frac{1}{|t|}f_{\mathcal{H}_f,\mathcal{H}_b}\left(t,\frac{h}{t};\rho\right)dt, \tag{7}$$

$$= \frac{1}{2\tilde{\rho}\sigma_f^2\sigma_b^2}\mathcal{I}_0\left(\frac{\rho\sqrt{h}}{\tilde{\rho}\sigma_f\sigma_b}\right)\mathcal{K}_0\left(\frac{\sqrt{h}}{\tilde{\rho}\sigma_f\sigma_b}\right), \tag{8}$$

where $\mathcal{K}_0(x) = \int_0^{\infty}\cos(x\sinh(t))dt$,is the zeroth order modified Bessel function of second kind. Also, the assumption $\mathbb{E}(\mathcal{H}_f) = \mathbb{E}(\mathcal{H}_b) = 1$ implies that $\sigma_f^2 = \sigma_b^2 = \frac{1}{2}$. It is obvious from Eq.(8) that obtaining the complementary CDF which is required for subsequent coverage analysis is quite involved. This significantly effects the tractability of the analysis and therefore analysis even when considering a single AP requires several folds of complex numerical integrations as in [3]. To this end, this paper develops an alternative performance characterization framework by developing a tight approximation for the PDF in (8).

Proposition 1 [Montonicity of Product]: Let $\mathcal{I}_v$ and $\mathcal{K}_v$ be the modified Bessel functions of first and second kind of order v, then their product $x \Rightarrow P_v(x) = \mathcal{I}_v(x)\mathcal{K}_v(x)$ is monotonically decreasing on the interval $(0,\infty)$. Also following bounds hold from asymptotic Hankel expansion

$$\mathcal{I}_v(x) \sim \frac{\exp(x)}{\sqrt{2\pi x}}\left(1+\mathrm{O}(x^{-1})\right), \tag{9}$$

$$\mathcal{K}_v(x) \sim \frac{\sqrt{\pi}\exp(-x)}{\sqrt{2x}}\left(1+\mathrm{O}(x^{-1})\right). \tag{10}$$

Detailed proof on the monotonicity of the product $P_v(x)$ can be found in [12]. Also by simulating the PDF from Eq. (8) it can be observed that $P_v(x)$ decreases exponentially fast, i.e., bounds obtained by using asymptotic expansion may be sufficient with appropriate scaling. Consequently, Eq. (8) can be written as

$$f_{\mathcal{H}}(h) = \frac{2}{\tilde{\rho}}\mathcal{I}_0\left(\frac{2\rho\sqrt{h}}{\tilde{\rho}}\right)\mathcal{K}_0\left(\frac{2\sqrt{h}}{\tilde{\rho}}\right), \tag{11}$$

$$\leq \underbrace{\frac{1}{2}\frac{\exp\left(\frac{-2(1-\rho)}{\tilde{\rho}}\sqrt{h}\right)}{\sqrt{\rho}\sqrt{h}}}_{\bar{f}_{\mathcal{H}}(h)}. \tag{12}$$

The bound in Eq.(12) can be converted into a proper PDF by selecting a normalization constant c such that $\int_0^{\infty}\bar{f}_{\mathcal{H}}(h)\,dh = c^{-1}$. Consequently, the PDF of $\mathcal{H} = \mathcal{H}_f\mathcal{H}_b$ can be approximated as

$$\text{PDF:} \quad f_{\mathcal{H}}^a(h) = \frac{\mu_1}{2}\frac{\exp\left(-\mu_1\sqrt{h}\right)}{\sqrt{h}}, \tag{13}$$

$$\text{CDF:} \quad F_{\mathcal{H}}^a(h) = 1-\exp\left(-\mu_1\sqrt{h}\right), \tag{14}$$

where $\mu_1 = \frac{2}{1+\rho}$ and consequently $\mathbb{E}(\mathcal{H}) = 2/\mu_1^2$ is the mean of the distribution. Comparing Eq.(13) with Eq. (2) from [3], it can be noticed that this approximation becomes precise as $\rho \to 1$. Computation of Kullback-Leibler (KL) divergence is a well known method to quantify the difference between two PDFs. Fig. 2 presents KL divergence between the exact PDF (see (8)) and the approximation established in Eq. (13). The intuitive conclusion that approximation error $\epsilon \to 0$ as the $\rho \to 1$ can be easily validated from the fig. 2 . Also it is obvious that even when $\mathcal{H}_f$ and $\mathcal{H}_b$ possess weaker correlation (i.e., $\rho \to 0$) the approximation performs reasonably well (for instance, refer to the fig. 2 for $\rho = 0.2$). It is worth highlighting that the rate at which KL divergence decreases exponentially fast with increasing ρ.

B. Coverage Probability for RF Backscatter WSN

In the following discussion, we will derive closed-form bounds on the coverage probability for a backscatter SN by

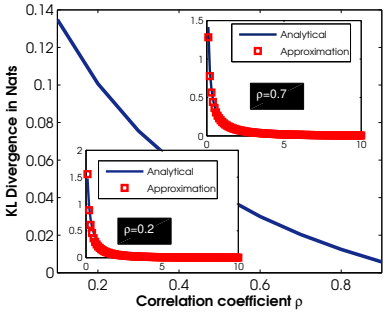

Fig. 2. Accuracy of the approximation in Eq. (13) vs. the exact PDF in Eq. (8) for varying correlation coefficient ρ using KL divergence.

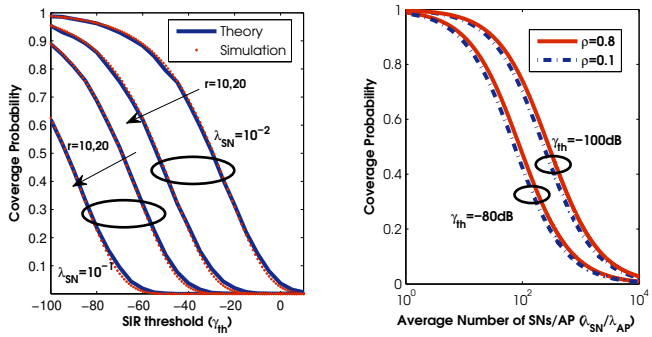

(a) Conditional coverage probability with varying desired SIR threshold (γ_{th}), link distance (r) and SN density (λ_{SN}) for the fixed $\rho = 0.5$ and $\alpha = 4$ (see Eq. (16)).

(b) Coverage probability for varying SN to AP ratio ($\tilde{\lambda}$) and channel correlation (ρ) for $\alpha = 4$ (see Eq. (17)).

Fig. 3. Validation of Results and Impact of Parametric variations on Coverage Probability.

exploiting the approximations developed in the previous subsection. Due to ergodicity of the HPPP, it is sufficient to characterize the performance of a typical link SN-AP link [13]. Consequently, the coverage probability of an arbitrary SN associated with the AP at the origin (without loss of generality) can be defined using Eq. (1) as

$$p_c\left(\gamma_{th}\right) \overset{(a)}{=} \mathbb{E}_R\left[\underbrace{\Pr\left\{\frac{\overbrace{l^2(r)\mathcal{H}_f^o\mathcal{H}_b^o}^{\Gamma}}{\sum_{j\neq o\in\Pi_{SN}} l^2(r_j)\mathcal{H}_f^j\mathcal{H}_b^j} \geq \gamma_{th}\right\}}_{p_c(\gamma_{th}|r)}\right], \quad (15)$$

where (a) assumes that the operation of considered link is interference limited, i.e. aggregate interference power is significantly larger than the noise variance, R is the random variable which captures the distance between AP and its intended SN with distribution: $f_R(r) = 2\pi r\lambda_{Ap}\exp\left(-\lambda_{AP}\pi r^2\right)$.

Proposition 2 [Coverage Probability]: The coverage probability of a SN located at a distance r from the transmitter can be upper-bounded as:

$$p_c\left(\gamma_{th}|\, r\right) \lessapprox \exp\left(-\lambda_{SN}\pi\mu_1^{\delta}\gamma_{th}^{\delta/2}\Gamma(1-\delta)\mathbb{E}(\mathcal{H}^{\delta})r^2\right), \quad (16)$$

where $\delta = 2/\alpha$ and $\mathbb{E}(\mathcal{H}^{\delta}) = \mathbb{E}(\mathcal{H}_f^{\delta}\mathcal{H}_b^{\delta})$ and $\Gamma(x)$ is the Gamma function. The unconditional coverage probability can be quantified by deconditioning $p_c\left(\gamma_{th}|\, r\right)$ by employing PDF of R as:

$$p_c\left(\gamma_{th}\right) \approx \frac{1}{1+\tilde{\lambda}\mu_1^{\delta}\gamma_{th}^{\delta/2}\Gamma(1-\delta)\mathbb{E}(\mathcal{H}^{\delta})}, \quad (17)$$

where $\tilde{\lambda} = \lambda_{SN}/\lambda_{AP}$ is the average number of SNs per AP.

Due to space limitations, we will not provide the complete proof. The key idea behind the proof is summarized in Appendix A. While we employ approximation for the CDF to characterize the fading on the intended link between AP and SN, this approximation is not required for the interfering link as all we need is the joint moments of the dependent exponential random variables $\mathbb{E}(\mathcal{H}^{\delta}) = \mathbb{E}(\mathcal{H}_f^{\delta}\mathcal{H}_b^{\delta})$. Middleton in [7] derived the expression for the joint moments $\mathbb{E}(\mathcal{H}_f^n\mathcal{H}_b^m)$, which is presented in Chapter 9, Eq. (9.22). However, this result is incorrect and for special cases such as $n = m = 1$, it does not yield the results presented in Eq. (9.23) of the same book. Since, detailed derivation is not provided, it is difficult to establish the error. In this article, we derive an expression for $\mathbb{E}(\mathcal{H}_f^n\mathcal{H}_b^m)$ from the joint distribution (see Eq. (6)) in Appendix B.

Proposition 4 [Joint Moments]: The joint moments of correlated bivariate Exponential random variable with correlation factor ρ can be computed as:

$$\begin{aligned}\kappa_{\mathcal{H}}\left(n,m\right) &= \mathbb{E}\left[\mathcal{H}_f^n\mathcal{H}_b^m\right], \\ &= \frac{\tilde{\rho}\Gamma(n+1)\Gamma(m+1){}_2\mathcal{F}_1\left(n+1,m+1,1;\rho^2\right)}{\Omega_f^n\Omega_b^m}, \\ &= 2^{n+m}\left(1-\rho^2\right)^{n+m+1}\sigma_f^{2n}\sigma_b^{2m}\Gamma(n+1) \\ &\times \Gamma(m+1){}_2\mathcal{F}_1\left(n+1,m+1,1;\rho^2\right). \quad (18)\end{aligned}$$

where $\Gamma(x)$ is the Gamma function and ${}_2\mathcal{F}_1\left(a,b,c;z\right)$ is the Gauss hypergeometric function.

IV. Results & Discussion

In this section, we validate the developed statistical framework for quantifying the coverage probability. We also briefly explore the impact of different parametric variations on the coverage probability. **1. Validation of the Developed Statistical Framework:** Fig. 3a corroborates the accuracy of the bounds presented in Eq. (16) with the help of Monte Carlo simulations. Monte Carlo simulation results are obtained by simulating 10^3 realizations of Π_{AP} and fading channels for each value of the desired SIR threshold (γ_{th}). As indicated by the Fig. 3a, the developed bounds closely match with the Monte Carlo simulations. It can be observed that the coverage probability of SN decreases with increase in the link distance (r) and density of sensor nodes (λ_{SN}), where the former is experienced due to the increased bi-directional path-loss and later can be attributed to the increased aggregate interference. **2. Average Number of SNs per AP:** Fig. 3b depicts the unconditional coverage probability (from Eq.

(17)) against varying ratio $\tilde{\lambda} = {}^{\lambda_{SN}}/_{\lambda_{AP}}$ which effectively captures the average number of SNs per AP. As demonstrated in Fig. 3b, the average number of SNs which can typically be supported for the desired SIR thresholds for a coverage probability of 90% is around 10-20. As expected the coverage probability decreases with increasing number of SNs per AP due to interference aggregation. The effective number of SNs per AP can be increased by introducing a medium access control (MAC) mechanism on backscattering nodes. As the SNs are passive devices, MAC implementation has only finite degrees-of-freedom for exploitation. These include polarization, channelization (through modulation of the period of data waveform which derives load modulation) or random ALOHA type scheduling. Extensive investigation of these mechanism is deferred for a future study.

V. Conclusions

In this paper, we developed a statistical framework to quantify the performance of backscatter communication based low power wireless sensor network. In particular, we developed novel closed-form bounds to characterize the coverage probability of SNs under dyadic Rayleigh fading channel and spatial randomness in topology. Compared to the existing literature, the developed bounds are simple and do not require several folds of numerical integration for performance evaluation. The tightness of the bounds is verified using Monte Carlo simulations. Lastly, we demonstrate that the developed framework can be exploited to dimension a backscattering based sensor network for the required QoS parameters.

Appendix A
Upper-bound on the Coverage Probability

The upper-bound on conditional coverage probability can be obtained by first computing the Laplace transform of the interference which indicates that the interference has an α-stable distribution and its PDF can be expressed as:

$$f_I(x) = \sum_{i=1}^{\infty} \frac{(-1)^{i+1}\Gamma(1+i\delta)\sin(\pi i\delta)\left(\frac{\lambda_{SN}\pi\Gamma(1-{}^{1}/_{\alpha})\mathbb{E}(\mathcal{H}^{{}^{1}/_{\alpha}})}{x^{{}^{1}/_{\alpha}}}\right)^{i}}{\pi x i!}. \tag{19}$$

The derivation follows a similar process to Chapter 3, Section 3.2 in [13] with modification of channel gains and path-loss exponents. Now employing Eq. (14), the conditional coverage probability can be expressed as:

$$\begin{aligned} p_c\left(\gamma_{th}|\, r\right) &= \mathbb{E}_I\left[\Pr\left\{\mathcal{H} \geq \gamma_{th} I l(r)^{-2}\right\}\right], \\ &= \int_0^{\infty} \exp\left(-\mu_1\sqrt{x\gamma_{th}l(r)^{-2}}\right) f_I(x)dx. \end{aligned} \tag{20}$$

Eq. (20) is simplified to Eq. (16) by evaluation of the integral, bounding one of the terms in intermediate steps, i.e. $\Gamma(1-2\delta i) \lessapprox \Gamma(1-\delta i)$ and then using $\exp(-x) = \sum_{i=0}^{\infty} \frac{x^i}{i!}$.

Appendix B
Derivation of Joint Moments

Employing the joint PDF from Eq. (6)., the (n,m) order moment $\kappa_{\mathcal{H}}(n,m) = \mathbb{E}\left[\mathcal{H}_f^n \mathcal{H}_b^m\right]$ can be computed as follows

$$\kappa_{\mathcal{H}}(n,m) = \int_0^{\infty}\int_0^{\infty} h_f^n h_b^m f_{\mathcal{H}_f,\mathcal{H}_b}(h_f,h_b;\rho)\, dh_f dh_b. \tag{21}$$

Let $\Omega_f = \left(2\tilde{\rho}\sigma_f^2\right)^{-1}$ and $\Omega_b = \left(2\tilde{\rho}\sigma_b^2\right)^{-1}$, then Eq. (21) can be re-written as

$$\begin{aligned} \kappa_{\mathcal{H}}(n,m) = \Omega_b\Omega_f\tilde{\rho}\int_0^{\infty} h_b^m \exp\left(-\Omega_b h_b\right) \\ \times \underbrace{\int_0^{\infty} h_f^n \exp(-\Omega_f h_f)\mathcal{I}_0\left(2\rho\sqrt{\Omega_b h_b}\sqrt{\Omega_f h_f}\right) dh_f}_{I_1}\, dh_b. \end{aligned} \tag{22}$$

Now, exploiting the infinite series expression for the modified Bessel function of first kind, I_1 can be evaluated as

$$I_1 = \sum_{k=0}^{\infty} \frac{\left(\rho^2\Omega_b h_b\right)^k}{\Gamma(k+1)\Gamma(k+1)} \frac{\Gamma(n+k+1)}{\Omega_f^{n+1}}. \tag{23}$$

Substituting, Eq. (23) into Eq. (21)

$$\kappa_{\mathcal{H}}(n,m) = \frac{\tilde{\rho}}{\Omega_f^n\Omega_b^m}\sum_{k=0}^{\infty}\frac{\Gamma(n+k+1)\Gamma(m+k+1)}{\Gamma(k+1)\Gamma(k+1)}\rho^{2k}. \tag{24}$$

Now using the definition of the rising factorial and the Guass hypergeometric function results in Eq. (24) completes the proof.

References

[1] B. Clerckx, R. Zhang, R. Schober, D. W. K. Ng, D. I. Kim, and H. V. Poor, "Fundamentals of wireless information and power transfer: From RF energy harvester models to signal and system designs," *IEEE Journal on Selected Areas in Communications*, vol. 1, 2018.

[2] A. Bletsas, P. N. Alevizos, and G. Vougioukas, "The art of signal processing in backscatter radio for ÎŒw (or less) internet of things: Intelligent signal processing and backscatter radio enabling batteryless connectivity," *IEEE Signal Processing Magazine*, vol. 35, pp. 28–40, Sep. 2018.

[3] C. Psomas and I. Krikidis, "Backscatter communications for wireless powered sensor networks with collision resolution," *IEEE Wireless Communications Letters*, vol. 6, pp. 650–653, Oct 2017.

[4] M. Bacha, B. Clerckx, and K. Huang, "Backscatter communications for the internet of things: A stochastic geometry approach," *CoRR*, vol. abs/1711.07277, 2017.

[5] N. Van Huynh, D. T. Hoang, X. Lu, D. Niyato, P. Wang, and D. I. Kim, "Ambient backscatter communications: A contemporary survey," *IEEE Communications Surveys & Tutorials*, vol. 20, no. 4, pp. 2889–2922, 2018.

[6] S. N. Chiu, D. Stoyan, W. S. Kendall, and J. Mecke, *Stochastic geometry and its applications*. John Wiley & Sons, 2013.

[7] D. Middleton, I. of Electrical, and E. Engineers, *An introduction to statistical communication theory*, vol. 960. McGraw-Hill New York, 1960.

[8] R. K. Mallik, "On multivariate rayleigh and exponential distributions," *IEEE Transactions on Information Theory*, vol. 49, no. 6, pp. 1499–1515, 2003.

[9] C. Tellambura and A. D. S. Jayalath, "Generation of bivariate rayleigh and nakagami-m fading envelopes," *IEEE Communications Letters*, vol. 4, no. 5, pp. 170–172, 2000.

[10] R. B. Ertel and J. H. Reed, "Generation of two equal power correlated rayleigh fading envelopes," *IEEE Communications Letters*, vol. 2, no. 10, pp. 276–278, 1998.

[11] M. K. Simon and M.-S. Alouini, *Digital communication over fading channels*, vol. 95. John Wiley & Sons, 2005.

[12] Á. Baricz, "On a product of modified bessel functions," *Proceedings of the American Mathematical Society*, vol. 137, no. 1, pp. 189–193, 2009.

[13] M. Haenggi, R. K. Ganti, *et al.*, "Interference in large wireless networks," *Foundations and Trends® in Networking*, vol. 3, no. 2, pp. 127–248, 2009.